analytical chemistry

Letter

Cite This: *Anal. Chem.* 2018, 90, 12356−12360

pubs.acs.org/ac

Quantitative Lateral Flow Strip Sensor Using Highly Doped Upconversion Nanoparticles

Hao He,[†,‡] Baolei Liu,[†] Shihui Wen,[†] Jiayan Liao,[†] Gungun Lin,[†,‡] Jiajia Zhou,[†] and Dayong Jin*[,†,‡]

[†]Institute for Biomedical Materials and Devices, Faculty of Science, University of Technology Sydney, Sydney, New South Wales 2007, Australia

[‡]ARC Research Hub for Integrated Device for End-user Analysis at Low-levels (IDEAL), Faculty of Science, University of Technology Sydney, Sydney, New South Wales 2007, Australia

Supporting Information

ABSTRACT: Paper-based lateral flow assays, though being low-cost and widely used for rapid in vitro diagnostics, are indicative and do not provide sufficient sensitivity for the detection and quantification of low abundant biomarkers for early stage cancer diagnosis. Here, we design a compact device to create a focused illumination spot with high irradiance, which activates a range of highly doped 50 nm upconversion nanoparticles (UCNPs) to produce orders of magnitude brighter emissions. The device employs a very low-cost laser diode, simplified excitation, and collection optics and permits a mobile phone camera to record the results. Using highly erbium ion (Er^{3+})-doped and thulium ion (Tm^{3+})-doped UCNPs as two independent reporters on two-color lateral flow strips, new records of limit of detection (LOD), 89 and 400 pg/mL, have been achieved for the ultrasensitive detection of prostate specific antigen (PSA) and ephrin type-A receptor 2 (EphA2) biomarkers, respectively, without crosstalk. The technique and device presented in this work suggests a broad scope of low-cost, rapid, and quantitative lateral flow assays in early detection of bioanalytes.

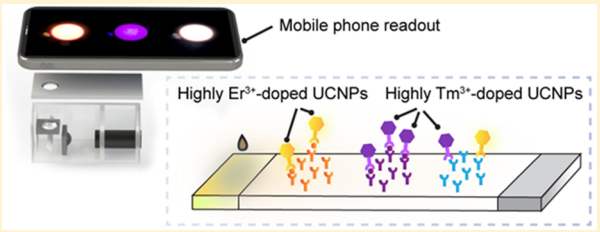

The simple and low-cost lateral flow strips (LFS), like pregnancy testing sticks, have been widely used for point-of-care applications, at home and clinics, without any training required. However, the current visually interpreted tests are indicative rather than quantitative, which are limited by their low visibility of the traditionally used reporters, such as colloidal gold nanoparticles[1] and dye encapsulated latex beads.[2] To overcome their inadequate sensitivity issue toward high performance in analytical assays and to meet the increasing demand in the quantitative detection of low abundance disease biomarker and toxins, new fluorescent nanoparticles are needed in LFS devices. Using semiconductor quantum dots[3] and ceramic upconversion nanoparticles (UCNPs),[4] fluorescence-based LFS sensors have high sensitivity. To do this, simple-to-use optical readers are also essential in fluorescence-based LFS sensors, as it not only produces quantitative results but also offers less subjective interpretation of results.

Another aspect that affects the detection sensitivity and accuracy in quantitative assays is the background noise, e.g., scatterings and autofluorescence of paper substrates under excitation illumination. For this reason, UCNPs have attracted more attention,[5−8] as they only require near-infrared excitation to emit signals in the visible wavelength range, in which case the autofluorescence from paper substrates is minimized. Moreover, different doping of lanthanide ions can produce a collection of choices of photostable multicolor emissions for high throughput multiplexed assays.[9]

In the early days, large UCNPs with a size of 400 nm were used in LFS sensors,[4] because a high brightness of emission signals is needed and large particles encapsulate a large number of emitters to meet this requirement. However, such big particles often block the pores of paper substrate and end up with higher noise from nonspecific blockage.[10] Enlarging pore size is not an option as the flow speed is too high to allow sufficient time for immunoassays; therefore, the pore size has to be within the range of a few micrometers to submicrometers scale in nitrocellulose strips.[11] Recently, controlled synthesis of small monodispersed UCNPs,[12] and at large quantity,[13] has been realized, and UCNPs in the range of tens of nanometers have been introduced for LFS sensors.[14] However, the intensity of smaller UCNPs drops significantly compared to the larger ones, due to the reduced volume of emitters and increased level of surface quenching. Therefore, LFS sensors using smaller UCNPs are often less sensitive, though UCNP-based strips have been suggested for the detection of analytes, such as *E. coli* (10^3 org/mL),[15] *Vibrio anguillarum* (10^2 cfu/mL),[16] cephalexin (0.6 ng/mL),[17] and prostate specific antigen (PSA, 556 ng/mL).[18] The key toward real world applications

Received: September 22, 2018
Accepted: October 12, 2018
Published: October 18, 2018

DOI: 10.1021/acs.analchem.8b04330
Anal. Chem. 2018, 90, 12356−12360

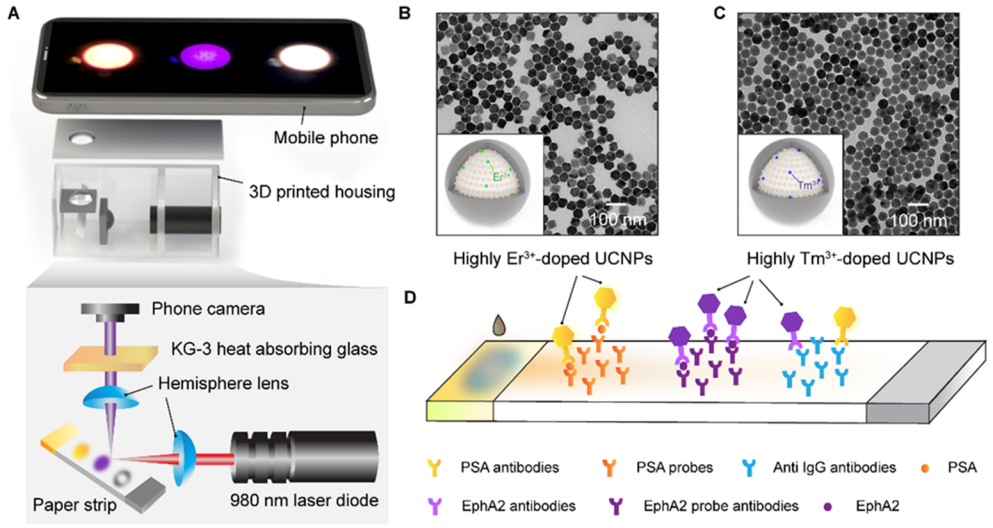

Figure 1. Schematic illustration of the LFS sensor: (A) A mobile phone-based reader and the optics layout. (B) Structure of highly Er^{3+}-doped core−shell UCNPs and the corresponding TEM image. (C) Structure of highly Tm^{3+}-doped core−shell UCNPs and the corresponding TEM image. (D) Two-color LFS assays for PSA and EphA2 analytes.

of UCNP-based LFS sensors is to significantly improve their limit of detection (LOD).

Instead of using large crystal host to increase the number of emitters, we have recently developed strategies to increase the concentration of emitters within small nanocrystals and to produce a range of highly doped UCNPs displaying exceptional brightness and sensitivity.[19−21] Conventionally, the doping level has been kept relatively low to ensure a sizable separation between the dopants to prevent parasitic interaction, which limits the concentration of dopants. To overcome the issue of concentration quenching of upconversion luminescence, we use a high irradiance, either by using a high-power laser or by focusing the excitation beam, and an inert shell passivation, to alleviate the threshold of concentration quenching, which ensures that each highly doped UCNP is exceptionally bright, sufficient for naked eye inspection through a simple microscope.[22]

On the other hand, the small cameras built in the smartphone have enabled the increased capabilities and ubiquity of smartphones to be used for point-of-care applications.[23] Together with the fast growing fields of low-cost laser diode and 3D-printing technologies, compact and low-cost readers can be made for fluorescence-based LFS sensors for quantification of low abundant biomarkers, but the sensitivity of phone cameras is yet to be improved.

In this study, we apply two kinds of UCNPs, highly doped by Er^{3+} ions to emit yellowish upconversion emissions and Tm^{3+} ions to emit purple upconversion emissions, as multicolor reporters in LFS. We print a plastic holder that aligns a low-cost excitation laser diode and collection optics (Figure 1), with a total cost of less than $100. The key is to tightly focus the excitation beam to only illuminate a small region on the paper substrate, which unlocks the high brightness of highly doped UCNPs to deliver high sensitivity detection of a smaller volume of samples. We demonstrate here that highly doped UCNPs provide significantly higher brightness than the conventional UCNPs, which allows a limit of detection of 89 pg/mL for PSA and 400 pg/mL for ephrin type-A receptor 2 (EphA2) achieved in a quantitative multiplexed assay without crosstalk.

To obtain smaller and brighter UCNPs, we synthesize two kinds of inert shell passivated UCNPs highly doped with Er^{3+} and Tm^{3+}, i.e., $NaYF_4$:8%Er/60%Yb@$NaYF_4$ and $NaYF_4$:8% Tm/60%Yb@$NaYF_4$, and evaluate their performance against the conventional UCNPs with the same size, i.e., $NaYF_4$:2%Er/20%Yb and $NaYF_4$:0.5%Tm/20%Yb (the synthesis methods are provided in SI Section 1). We use a ligand exchange method to modify the surfaces of UCNPs with carboxyl groups, followed by an EDC/NHS method to conjugate antibodies (as shown in SI Section 2). The uniformity of each UCNP sample is confirmed by TEM characterization shown in Figure 1B,C, and SI Section 3. The successful conjugation of antibodies is confirmed by UV absorption spectra with a characteristic peak appearance at 280 nm and the dynamic light scattering revealing a slight increase in size (as shown in SI Section 4).

We particularly test the power dependent properties of the as-prepared UCNPs reporters, in terms of their emission intensities and spectrum profiles using a purpose-built single nanoparticle characterization system.[22] As shown in Figure 2A, the brightness of highly doped UCNPs increases much more significantly than the lower doped ones with increasing excitation power density. The enhancement ratios of the emission brightness for highly Er^{3+}- and Tm^{3+}-doped UCNPs are 5 times and 12 times more than that of lower doped ones when the power reaches above 0.5 MW/cm^2. As shown in Figure S3, the emission spectrum of highly Er^{3+}-doped UCNP reporters emits a lot more intensity in red around 650 nm under higher excitation power, which results in a bright yellowish emission. This paint mixing effect also happens in the highly Tm^{3+}-doped UCNP reporters with appearance in purple from the phone camera (power dependent spectrum profiles of four UCNP reporters are shown in SI Section 5).

To quantify the higher brightness of highly doped UCNPs as reporters on LFS, we compare highly Er^{3+}-doped UCNP reporter and a lower doped one by detecting different concentrations of target PSA using lateral flow strips (the details of strip fabrication and LFS assay are shown in SI Sections 6 and 7). Under an excitation power density of 0.5 MW/cm^2, the signals from test area and background area are

DOI: 10.1021/acs.analchem.8b04330
Anal. Chem. 2018, 90, 12356−12360

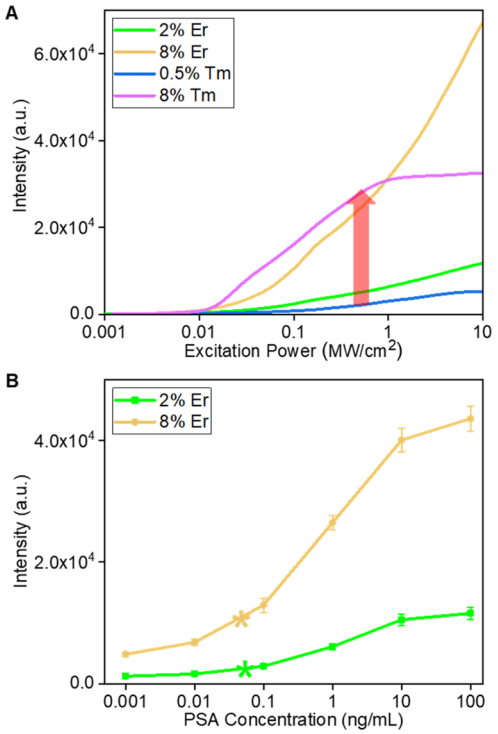

Figure 2. (A) Power dependent emission intensity profiles of single highly doped UCNP reporters and lower doped ones on glass slides. The red arrow indicates the power density at 0.5 MW/cm^2. (B) The fluorescence signal intensities of test area on strips for detecting different concentrations of PSA using highly Er^{3+}-doped UCNP reporters and lower doped ones tested by a single photon counting detector. Each data point represents the mean (±standard deviation) of triplicate experiments, and the stars mark the LODs.

recorded by a single photon counting detector (the optical layout is illustrated in SI Section 8). As shown in Figure 2B, the highly doped UCNP reporters show much higher signal compared to the lower doped ones and the brightness enhancement ratio is consistent with the single nanoparticle characterization results. Despite the difference in the brightness, both reporters show the same limit of detection of 50 pg/mL for PSA (LOD in this work is defined as the target concentration where the intensity is equal to the sum of background noise and three times the standard deviation above the background noise, and the details of calculation are shown in SI Section 9). The lower doped UCNP reporters require the use of a highly sensitive and costly single photon counting detector, which is not suitable for point-of-care applications. Only the highly doped UCNP reporters provide sufficient brightness for a normal phone camera to achieve the high sensitivity.

We build a compact device enclosed by a 3D-printed small housing as shown in Figure 1. The device consists of a 300 mW, 980 nm laser diode as the light source, two hemisphere lenses with one to focus the excitation light beam to the strip and the other for collecting the emission signal to the phone camera, and a low-cost KG-3 heat absorbing glass as the short pass filter to remove the laser scattering. The spectral response of the phone camera CMOS (Sony IMX-214, the most commonly used one)[24] and the transmission curve of the KG-3 glass[25] (as shown in SI Section 10) indicate that the phone camera can read most of the visible emission signals of our highly doped UCNP reporters with a negligible amount of excitation scattering light detected.

To read the strip, we fix the optics and camera setting and move the strip from one side to the other at a constant speed, so that the average fluorescence intensity values of the testing area, the control area, and the background area can be extracted from video analyses (Figure 3A and SI Section 11).

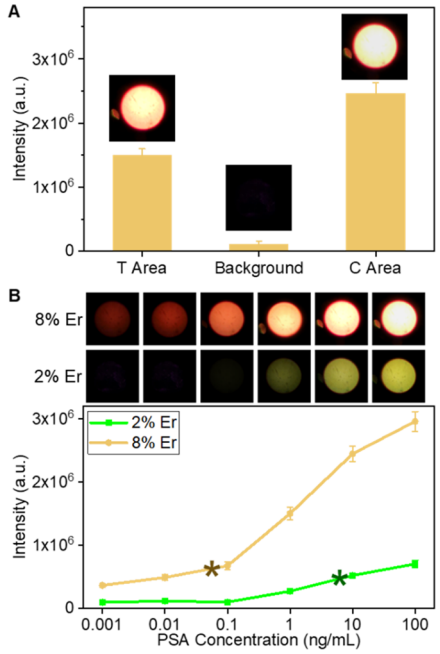

Figure 3. (A) A representative result from a typical PSA assay showing the signals from testing area, background, and control area. (B) Result photos and fluorescence intensities of testing areas for detecting different concentrations of PSA using highly Er^{3+}-doped UCNP reporters and lower doped ones. Each data point represents the mean (±standard deviation) of triplicate experiments, and the stars mark the LODs.

Using this method, Figure 3B shows the advantage of highly doped UCNP reporters when the target concentration is at a very low range where the lower doped UCNP group shows no detectable signals. The LOD for PSA using highly Er^{3+}-doped UCNP reporters is 61 pg/mL, more sensitive than using the lower doped ones (LOD: 8.5 ng/mL). The value of LOD suggests better performance of the highly doped UCNP-based LFS assay for PSA detection than previously reported LFS assays using conventional UCNP reporters (556 ng/mL)[18] as well as the one using commercial dissociation-enhanced lanthanide fluoroimmunoassay (DELFIA) kits (100 pg/mL).[26] There have been reported ultrasensitive nanoparticle-based PSA detection with LOD as low as 0.5 pg/mL by using a small nanoprobe in the DELFIA kit;[27] however, our LFS assay affords a lower-cost and simpler-to-use way.

To show the potential of the smart phone-based quantitative LFS for multiplexed assays, we use both highly Er^{3+}- and Tm^{3+}-doped UCNP reporters in a single strip for simultaneous testing of PSA and EphA2 target analytes. To achieve this, we modify highly Er^{3+}-doped UCNPs with anti-PSA antibodies and highly Tm^{3+}-doped UCNPs with anti-EphA2 antibodies. Figure 4A shows the results of testing the two targets. The yellowish and purple colors indicate the existence of PSA and EphA2, respectively, and their brightness increases along with

DOI: 10.1021/acs.analchem.8b04330
Anal. Chem. 2018, 90, 12356−12360

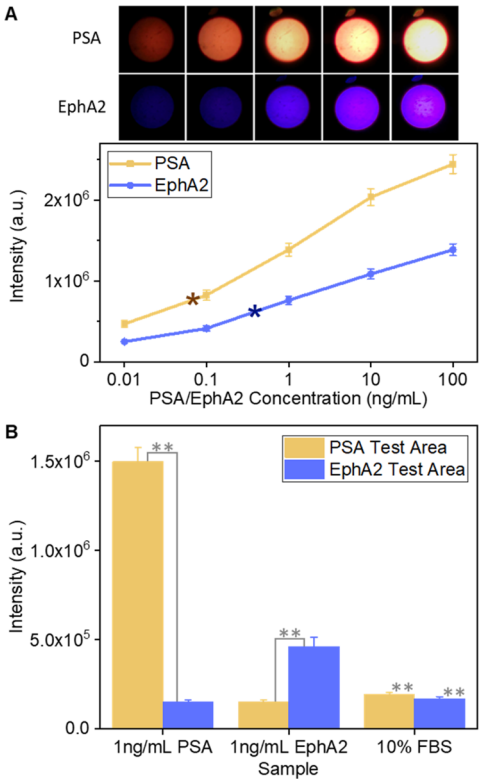

Figure 4. (A) Photos and fluorescence intensities of testing areas of the two-color LFS assay for testing different concentrations of PSA and EphA2. (B) Specificity evaluation of two-color LFS for 1 ng/mL PSA and EphA2 and 10% FBS. Each data point and bar represents the mean (±standard deviation) of triplicate experiments, and the stars mark the LODs. Significant difference is show with ** ($P < 0.01$).

the increase of concentrations of targets. This two-color LFS system achieves a LOD of 89 pg/mL for PSA (Figure 4A), which indicates this system maintains the high sensitivity as compared with a single-color one. The LOD for EphA2 is 400 pg/mL (Figure 4A). As the emission energy of highly Tm^{3+}-doped UCNP reporters is mainly around 800 nm (Figure S3D), which is beyond the range of detection optics and phone camera (Figure S5), the signal intensity is lower. We further evaluate the specificity of such a two-color LFS system by testing two targets PSA and EphA2 separately with 10% fetal bovine serum (FBS) as an interfering sample. Compared to the control groups, all the positive groups show much higher intensity with a significant difference ($P < 0.01$). The results indicate that there is negligible cross-interactions.

The rapid progress in material science provides a large library of bright nanoparticles for biomolecular assays. The highly doped UCNPs, employed in this work, have presented major advances in this field of applications, due to their high brightness, monodispersity, and uniformity in size and intensity, as well as being able to emit tunable colors according to the design of synthesis. Continuous development of more efficient and size controllable nanoparticle reporters will further improve the detection sensitivity in smart phone-based POCT applications. The quality of camera and the speed of CPU, built in smart phones, will continue to be improved and support more sophisticated image analysis and data processing, which shows a huge potential to drive the field of POCT from being indicative to being quantitative and user-friendly. On the other hand, the accuracy of biomarker-based cancer diagnostics will be primarily improved by increasing the number of biomarkers being simultaneously tested. Therefore, the capacity of multiplexed LFS assays will play an essential role, which accordingly demands the development of both multicolor reporters and the capacity of the phone camera to decode these colors.

In conclusion, we have designed a quantitative LFS sensor using highly doped UCNPs as reporters and a phone camera as the readout element. The device eliminates the use of a costly single photon counting detector and retains the high sensitivity of detecting low-abundance target analyte. We have achieved a LOD of 61 pg/mL for PSA. By designing two types of highly doped UCNPs emitting two different colors as reporters, the sensor can simultaneously detect PSA and EphA2 with a LOD of 89 and 400 pg/mL, respectively, without crosstalk. This portable device with ultrabright luminescent reporters could be potentially applied in detecting a wide range of biomarkers for early diagnostics or competitive assays for a broader range of analytical applications.

■ ASSOCIATED CONTENT

Supporting Information

The Supporting Information is available free of charge on the ACS Publications website at DOI: 10.1021/acs.analchem.8b04330.

Synthesis of UCNPs; bioconjugation of UCNPs with antibodies; TEM characterization; UV absorption spectra and dynamic light scattering; power dependent spectra; fabrication of paper-based strip; LFS assay for detecting target; strip test system based on SPAD; calculation of LOD; spectral response of the phone camera CMOS and transmission curve of KG-3 glass; phone camera-based signal reading (PDF)

■ AUTHOR INFORMATION

Corresponding Author

*E-mail: dayong.jin@uts.edu.au.

ORCID

Hao He: 0000-0003-3878-3349
Shihui Wen: 0000-0002-4670-4658
Jiajia Zhou: 0000-0002-0605-5745
Dayong Jin: 0000-0003-1046-2666

Notes

The authors declare no competing financial interest.

■ ACKNOWLEDGMENTS

The authors acknowledge the financial support from the China Scholarship Council (H.H.: No. 201504910696; B.L.: No. 201706020170; J.L.: No. 201508530231) and the Australian Research Council (ARC) Future Fellowship Scheme (D.J., FT130100517).

■ REFERENCES

(1) Choi, D. H.; Lee, S. K.; Oh, Y. K.; Bae, B. W.; Lee, S. D.; Kim, S.; Shin, Y.-B.; Kim, M.-G. *Biosens. Bioelectron.* **2010**, *25* (8), 1999−2002.
(2) Lee, S.; Mehta, S.; Erickson, D. *Anal. Chem.* **2016**, *88* (17), 8359−8363.
(3) Li, Z.; Wang, Y.; Wang, J.; Tang, Z.; Pounds, J. G.; Lin, Y. *Anal. Chem.* **2010**, *82* (16), 7008−7014.
(4) Hampl, J.; Hall, M.; Mufti, N. A.; Yao, Y. M.; MacQueen, D. B.; Wright, W. H.; Cooper, D. E. *Anal. Biochem.* **2001**, *288* (2), 176−187.

DOI: 10.1021/acs.analchem.8b04330
Anal. Chem. 2018, 90, 12356−12360

(5) Zhou, Y.; Chen, Y.; He, H.; Liao, J.; Duong, H. T. T.; Parviz, M.; Jin, D. *J. Rare Earths* **2018**, DOI: 10.1016/j.jre.2018.05.008.
(6) Chen, Y.; Duong, H. T. T.; Wen, S.; Mi, C.; Zhou, Y.; Shimoni, O.; Valenzuela, S. M.; Jin, D. *Anal. Chem.* **2018**, *90* (1), 663−668.
(7) Liu, C.; Chang, L.; Wang, H.; Bai, J.; Ren, W.; Li, Z. *Anal. Chem.* **2014**, *86* (12), 6095−6102.
(8) Zhou, J.; Leaño, J. L.; Liu, Z.; Jin, D.; Wong, K.-L.; Liu, R.-S.; Bünzli, J.-C. G. *Small* **2018**, *14* (40), 1801882.
(9) You, M.; Lin, M.; Gong, Y.; Wang, S.; Li, A.; Ji, L.; Zhao, H.; Ling, K.; Wen, T.; Huang, Y.; et al. *ACS Nano* **2017**, *11* (6), 6261−6270.
(10) Laitinen, M. P. A.; Vuento, M. *Biosens. Bioelectron.* **1996**, *11* (12), 1207−1214.
(11) Henderson, K.; Stewart, J. *J. Immunol. Methods* **2002**, *270* (1), 77−84.
(12) Liu, D.; Xu, X.; Du, Y.; Qin, X.; Zhang, Y.; Ma, C.; Wen, S.; Ren, W.; Goldys, E. M.; Piper, J. A.; et al. *Nat. Commun.* **2016**, *7*, 10254.
(13) You, W.; Tu, D.; Zheng, W.; Shang, X.; Song, X.; Zhou, S.; Liu, Y.; Li, R.; Chen, X. *Nanoscale* **2018**, *10* (24), 11477−11484.
(14) Liang, Z.; Wang, X.; Zhu, W.; Zhang, P.; Yang, Y.; Sun, C.; Zhang, J.; Wang, X.; Xu, Z.; Zhao, Y.; et al. *ACS Appl. Mater. Interfaces* **2017**, *9* (4), 3497−3504.
(15) Niedbala, R. S.; Feindt, H.; Kardos, K.; Vail, T.; Burton, J.; Bielska, B.; Li, S.; Milunic, D.; Bourdelle, P.; Vallejo, R. *Anal. Biochem.* **2001**, *293* (1), 22−30.
(16) Zhao, P.; Wu, Y.; Zhu, Y.; Yang, X.; Jiang, X.; Xiao, J.; Zhang, Y.; Li, C. *Nanoscale* **2014**, *6* (7), 3804−3809.
(17) Liu, C.; Ma, W.; Gao, Z.; Huang, J.; Hou, Y.; Xu, C.; Yang, W.; Gao, M. *J. Mater. Chem. C* **2014**, *2* (45), 9637−9642.
(18) Juntunen, E.; Arppe, R.; Kalliomäki, L.; Salminen, T.; Talha, S. M.; Myyryläinen, T.; Soukka, T.; Pettersson, K. *Anal. Biochem.* **2016**, *492*, 13−20.
(19) Ma, C.; Xu, X.; Wang, F.; Zhou, Z.; Liu, D.; Zhao, J.; Guan, M.; Lang, C. I.; Jin, D. *Nano Lett.* **2017**, *17* (5), 2858−2864.
(20) Wen, S.; Zhou, J.; Zheng, K.; Bednarkiewicz, A.; Liu, X.; Jin, D. *Nat. Commun.* **2018**, *9* (1), 2415.
(21) Zhao, J.; Jin, D.; Schartner, E. P.; Lu, Y.; Liu, Y.; Zvyagin, A. V.; Zhang, L.; Dawes, J. M.; Xi, P.; Piper, J. A.; et al. *Nat. Nanotechnol.* **2013**, *8*, 729.
(22) Wang, F.; Wen, S.; He, H.; Wang, B.; Zhou, Z.; Shimoni, O.; Jin, D. *Light: Sci. Appl.* **2018**, *7*, 18007.
(23) Shah, K. G.; Singh, V.; Kauffman, P. C.; Abe, K.; Yager, P. *Anal. Chem.* **2018**, *90* (11), 6967−6974.
(24) Sony Semiconductor Solutions Corporation. *IMX214*; https://www.sony-semicon.co.jp/products_en/new_pro/april_2014/imx214_e.html (Accessed Aug 30 2018).
(25) Edmund Optics. *12.5mm KG-3 Heat Absorbing Glass*; https://www.edmundoptics.com/p/125mm-dia-kg-3-heat-absorbing-glass/9438/ (Accessed Aug 30 2018).
(26) Järås, K.; Adler, B.; Tojo, A.; Malm, J.; Marko-Varga, G.; Lilja, H.; Laurell, T. *Clin. Chim. Acta* **2012**, *414*, 76−84.
(27) Xu, J.; Zhou, S.; Tu, D.; Zheng, W.; Huang, P.; Li, R.; Chen, Z.; Huang, M.; Chen, X. *Chem. Sci.* **2016**, *7* (4), 2572−2578.

DOI: 10.1021/acs.analchem.8b04330
Anal. Chem. 2018, 90, 12356−12360